CHEMIJA
2024. Vol. 35. No. 2. P. 35–44

ISSN 0235-7216 eISSN 2424-4538
DOI: https://doi.org/10.6001/chemija.2024.35.2.2

Initial evaluation of waste phosphogypsum for its use as a precursor for bioceramic materials

Elžbieta Bajorinaitė,

Laura Michailova,

Simona Jurevičiūtė,

Denis Sokol,

Živilė Stankevičiūtė,

Inga Grigoravičiūtė,

Aivaras Kareiva*

Institute of Chemistry,
Vilnius University,
24 Naugarduko Street,
03225 Vilnius, Lithuania

In this study, the phosphogypsum waste taken from various places in the factory dump located in Kėdainiai (Lithuania) was reinspected and characterised by different physico-chemical characterisation methods. The results of X-ray diffraction analysis, thermogravimetric analysis and differential scanning calorimetry, Fourier transform infrared spectroscopy, energy-dispersive X-ray analysis, elemental analysis using inductively coupled plasma optical emission and X-ray fluorescence spectroscopy confirmed that the main crystalline phase of the phosphogypsum waste is gypsum ($CaSO_4 \cdot 2H_2O$). The surface morphology of the investigated materials was analysed using scanning electron microscopy. The specific surface area was determined by the Brunauer–Emmet–Teller method. The pore size distribution of the material produced was obtained using the Barrett–Joyner–Halenda method. This study also demonstrated that the phosphogypsum waste could be successfully used as a precursor for the dissolution-precipitation synthesis of high quality bioceramic calcium hydroxyapatite.

Keywords: phosphogypsum, characterisation, bioceramic materials, dissolution-precipitation synthesis, calcium hydroxyapatite

INTRODUCTION

The majority of the extracted phosphorus compounds are utilised as fertilizers [1–3]. The company 'Lifosa' located in Kėdainiai (Lithuania) specialises in the production of phosphorus fertilizers, including diammonium phosphate, monocalcium phosphate and amonoammonium phosphate. The company itself synthesises phosphoric acid from apatites, which it subsequently employs in the process of fertilizer production [4]. During the synthesis of phosphoric acid, a by-product, phosphogypsum, is formed:

$$Ca_5(PO_4)_3X + 5H_2SO_4 + 2H_2O \rightarrow$$

$$3H_3PO_4 + 5CaSO_4 \cdot 2H_2O + HX. \quad (1)$$

Here X is OH, F, Cl and Br. Although it is claimed that phosphogypsum is a non-hazardous waste, it does not pose any danger to humans or the environment, and its chemical composition may vary depending on the origin of the phosphate raw material used in the technological process – apatite. In addition, huge amounts of phosphogypsum waste were generated on the territory of the factory – about 45 million tons. So, next to Kėdainiai several kilometres long 'phosphogypsum mountains' with a height of up to 80 m are deposited (see Fig. 1).

Globally, phosphogypsum is being tried to be used as a fertilizer, a construction material for building roads and equipping storage areas, as well as for growing meadow mushrooms [5–11]. However, the development and improvement of technologies for the efficient use of this raw material is still underway. The aim of this our

* Corresponding author. Email: aivaras.kareiva@chgf.vu.lt

Fig. 1. Phosphogypsum mountains located on the territory of AB 'Lifosa' factory

work is to once again reinspect and characterise the phosphogypsum waste derived from various places within the factory dump using a range of different physico-chemical characterisation methods and to propose the utilisation of phosphogypsum waste for synthesising artificial bone implants – high quality and low cost calcium hydroxyapatite ($Ca_{10}(PO_4)_6(OH)_2$; CHA). It is noteworthy that the dump is inhabited by vegetation and visited by wild animals. It is therefore reasonable to posit that this secondary raw material has the potential to serve as a precursor for the synthesis of high-quality biomaterials.

EXPERIMENTAL

Waste phosphogypsum, disodium hydrogen phosphate (Na_2HPO_4, 98%, Merck) and sodium dihydrogen phosphate (NaH_2PO_4, 99%, Merck) were used as starting materials for the fabrication of CHA powders via a dissolution-precipitation reaction. In the synthesis process, an initial 1.00 g portion of waste phosphogypsum was placed in the reaction vessel and mixed with a 100.0 mL solution of 1.00 M Na_2HPO_4 or with a mixture containing 50.0 mL of 1.00 M Na_2HPO_4 and 50.0 mL of 1.00 M NaH_2PO_4. The resultant mixture was left for 48, 96, 144 and 192 h allowing the reaction to progress in an oven at ~80°C temperature. After the synthesis, the liquid phase was decanted, and the resulting powders were rinsed with 500 mL of hot (~80°C) deionised water, followed by several additional rinses with 250 mL of room-temperature deionised water. Finally, the vacuum-filtered product was dried at 80°C for 2 h.

The prepared samples were characterised by powder X-ray diffraction (XRD) using a Rigaku MiniFlex II diffractometer with Cu Kα radiation (λ = 1.541838 Å). The diffraction data was obtained by scanning in the 2θ range of 10–60° at a scan speed of 2°/min. The thermal decomposition of the sample was examined by thermogravimetric analysis and differential scanning calorimetry (TG-DSC) using a Perkin Elmer STA 6000 Simultaneous Thermal Analyzer. Approximately 10 mg of the sample was heated from 25 to 900°C at a heating rate of 10°C/min in the flowing air atmosphere (20 mL/min). Fourier transform infrared spectroscopy (FT-IR) was performed using an Alpha spectrometer (Bruker, Inc., Germany) in the wavenumber range from 4000 to 450 cm^{-1}, with a resolution of 4 cm^{-1}. The product morphology was analysed using field-emission scanning electron microscopy (SEM, SU-70, Hitachi,

Tokyo, Japan). Energy-dispersive X-ray (EDX) analysis of the sample was performed using a SEM Hitachi TM 3000. An inductively coupled plasma optical emission spectrometer Perkin Elmer Optima 7000dv and a wave dispersion X-ray fluorescence analyzer WD-XRF Rigaku Supermini 200 were also used to determine the amount of metals. The specific surface area was measured by the Brunauer–Emmet–Teller (BET) method under vacuum for the degassed at 120°C sample by N_2 adsorption-desorption isotherm (at 77 K) using a Tristar II instrument (Norcross, GA, USA). The pore size distribution of the material produced was obtained using the Barrett–Joyner–Halenda (BJH) method.

RESULTS AND DISCUSSION

Powder XRD patterns of phosphogypsum samples taken from three different parts of collected waste are presented in Fig. 2. As illustrated in Fig. 2, the XRD patterns of the analysed phosphogypsum samples are nearly identical, regardless of the sampling location. The determined main crystalline phase is gypsum ($CaSO_4 \cdot 2H_2O$; PDF [96-500-0040]), and no even traces of side crystalline phases could even be detected from the XRD results. The sample may contain impurity crystalline phases, the amount of which is below the detection limit, or those extraneous phases are amorphous, for which the XRD method is not suitable for detection.

Again, the thermal behaviour for the samples collected at different parts of the waste is very similar. The TG/DTG/DSC curves of two representative phosphogypsum samples are shown in Fig. 3. The negligible weight loss observed below 50°C is attributed to the evaluation of adsorbed moisture. The main mass loss in a temperature range of 90–150°C and a very small weight loss in a range of 150–200°C are visible in the TG curves. In general, gypsum dehydration involves the two-step process [12]:

$$CaSO_4 \cdot 2H_2O \rightarrow CaSO_4 \cdot 0.5H_2O + 1.5H_2O\uparrow \rightarrow$$

$$CaSO_4 + 0.5H_2O\uparrow. \quad (2)$$

The TG curves revealed a total mass loss of 20.5–21.0% in the temperature range between 90 and 200°C, which approximately corresponds to the loss of two molecules of structural water (theoretical mass loss of 20.9%). According to Eq. (2), the theoretical value of the first mass loss should be equal to 15.7% with the formation of hemihydrate. The second mass loss attributed to the last

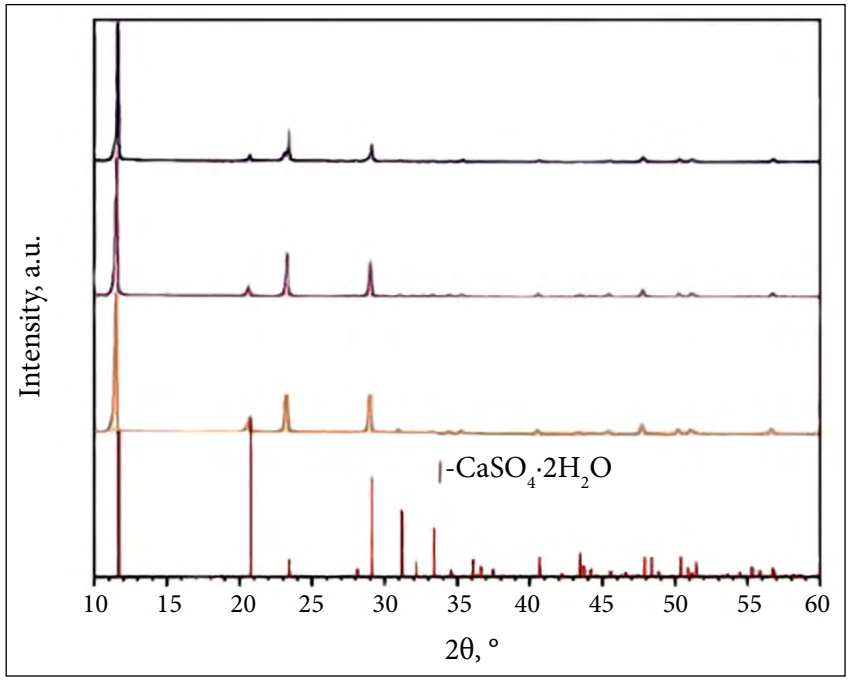

Fig. 2. XRD patterns of the phosphogypsum samples taken from three different parts of collected waste

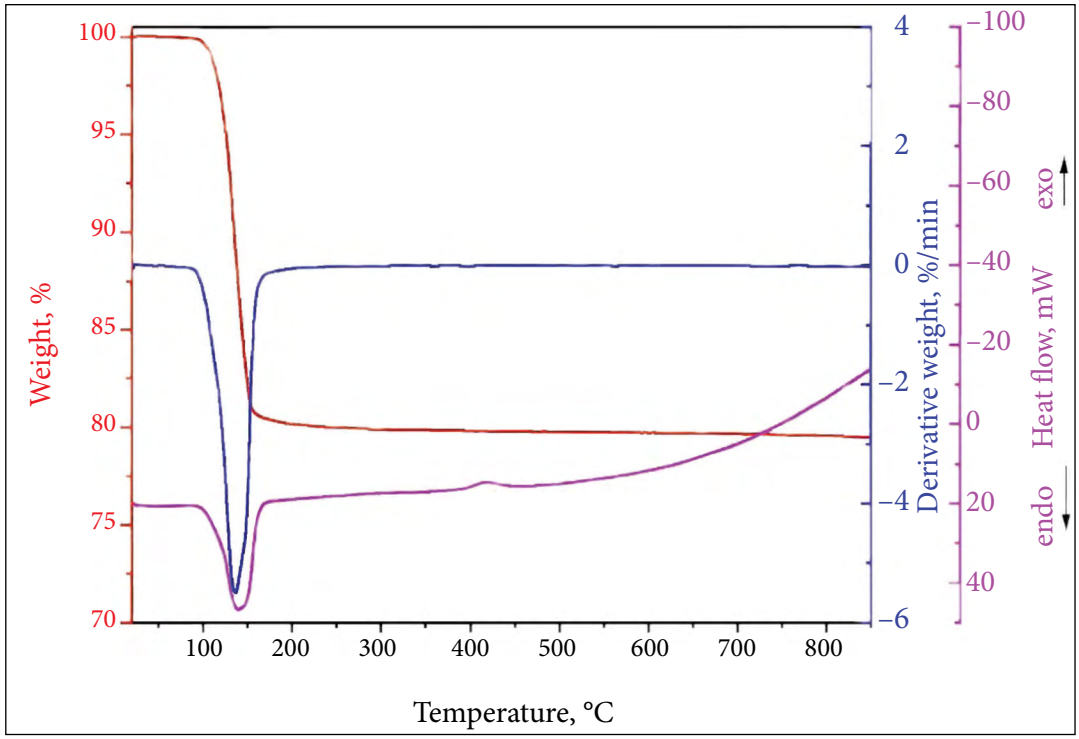

Fig. 3. The TG/DTG/DSC curves of a representative phosphogypsum sample. Sample weight was 10 mg, and the heating rate was 10°C/min under air atmosphere with a flow rate of 20 mL/min

dehydration reaction should be located at 150°C. However, the actual dehydration of phosphogypsum overlaps, thus indicating that hemihydrate begins to transform into soluble anhydrite before gypsum completely transforms into hemihydrate. Therefore, the three phases (gypsum, hemihydrate, and soluble anhydrite) would coexist during certain periods of dehydration.

Furthermore, two endothermic peaks were observed at approximately 150°C in the DSC curves. This endotherm could be assigned to the dehydration of gypsum. The low-intensity exothermic peaks at about 410°C could also be determined in the DSC curves. This peak is related to transforming soluble anhydrite to insoluble anhydrite (see Fig. 4).

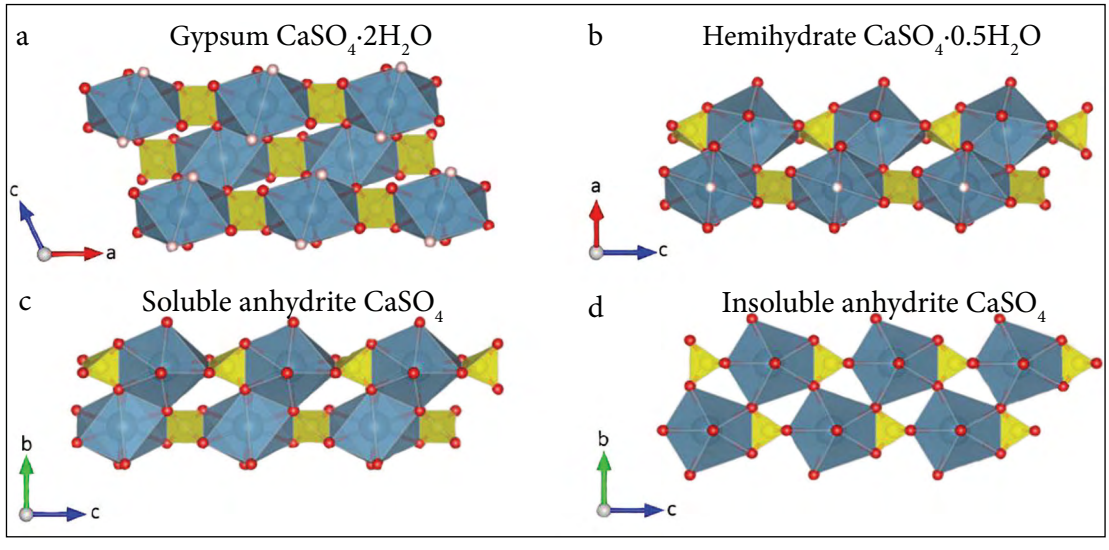

Fig. 4. Comparison of one-dimensional linear chains in (a) gypsum, (b) hemihydrate, (c) soluble anhydrite and (d) insoluble anhydrite

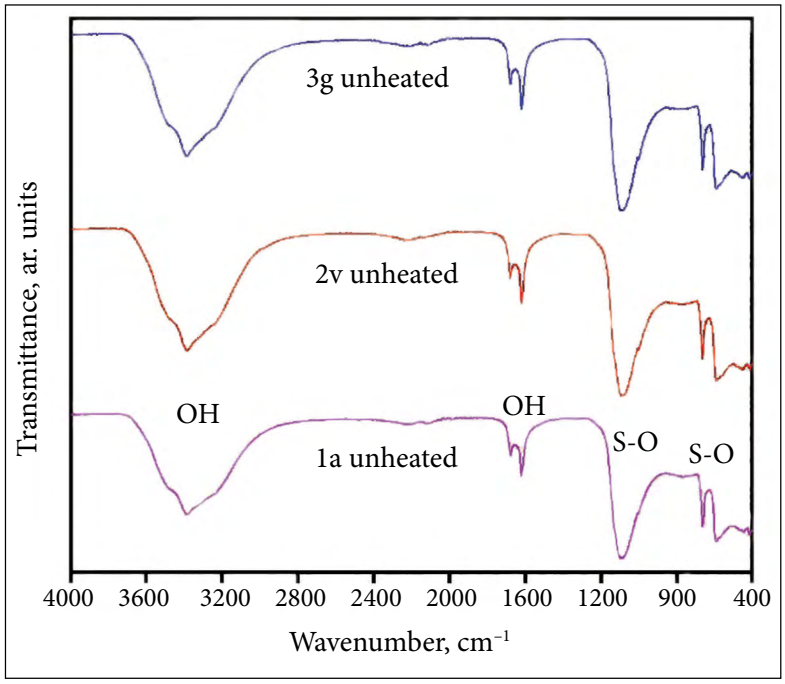

Fig. 5. FTIR spectra of the phosphogypsum samples taken from three different parts of collected waste

The FTIR spectra of phosphogypsum samples in a range of 4000–400 cm^{-1}, obtained from three different parts of the collected waste, are presented in Fig. 5. The strong absorption bands, which split into two components at approximately 1145 and 1115 cm^{-1}, and the small peaks at 670 and 600 cm^{-1}, which were determined in FTIR spectra, could be assigned to the stretching and bending modes of sulfate (SO_4^{2-}) in the pure gypsum (Fig. 5). The stretching vibrations of the OH in H_2O in the gypsum could be observed at 3580–3430 cm^{-1} and at 1680–1600 cm^{-1} [13]. Thus, the FTIR results are clearly supporting the conclusions made from the XRD analysis data.

The SEM micrographs of the phosphogypsum samples taken from different parts of collected waste are presented in Fig. 6. The surface of phosphogypsum is composed of large and differently oriented 20–30 μm in size plate-like crystals and microroads of $CaSO_4 \cdot 2H_2O$. The SEM images obtained at higher magnifications (Fig. 7) confirm that these large crystals are covered with smaller particles which could be attributed to some side phases.

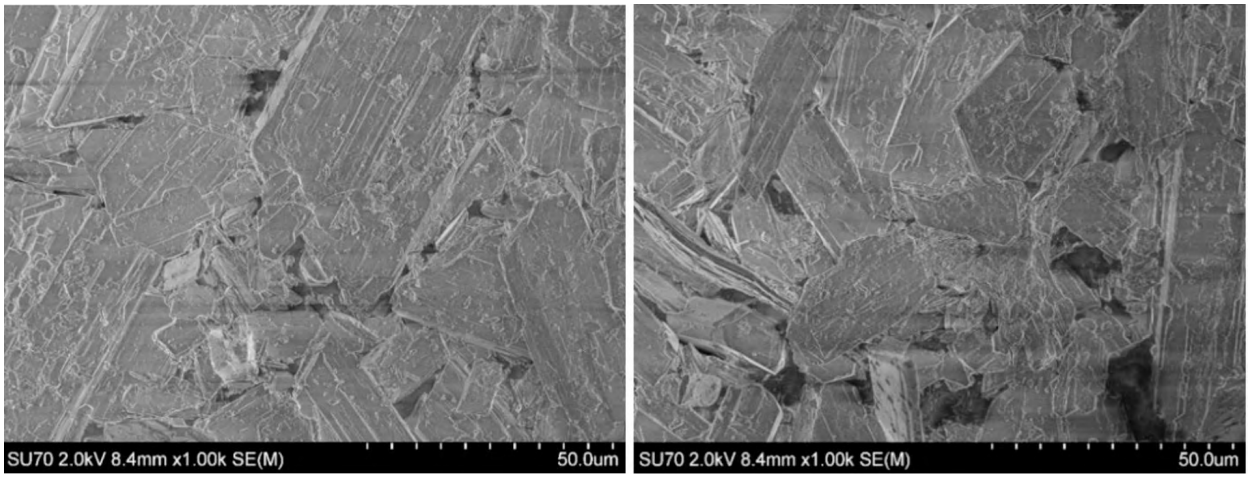

Fig. 6. SEM micrographs of the phosphogypsum samples taken from different parts of collected waste

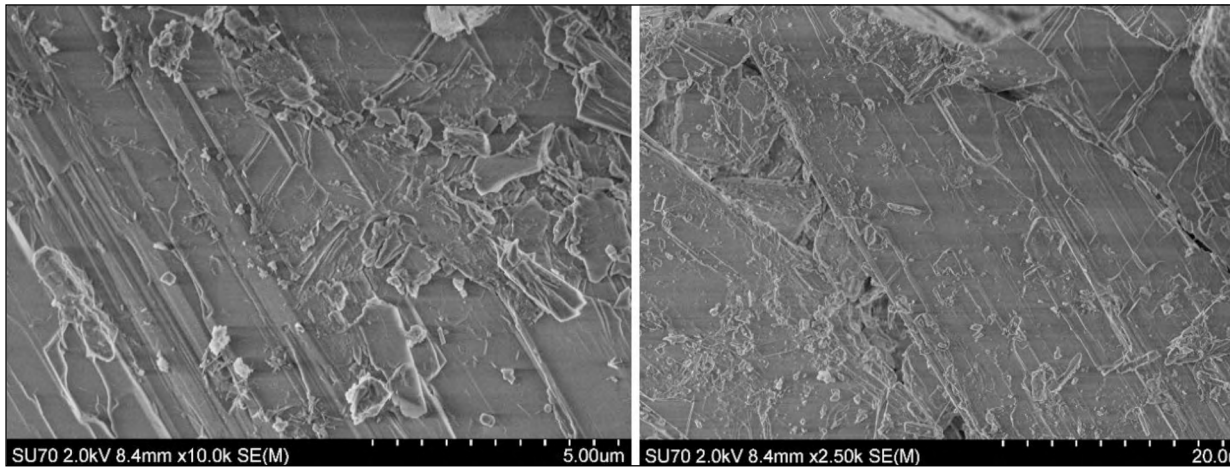

Fig. 7. SEM micrographs of the phosphogypsum obtained at higher magnifications

The results of EDX analysis confirmed that Ca and S are the main elements in phosphogypsum. The representative EDX spectrum is presented in Fig. 8. The calculated molar ratio of Ca:S was about 1. The small amount of Al, Si and P are also present in the analysed specimens of phosphogypsum. The AAS and XRF methods were also employed for the determination of a small amount of metals. The results of elemental analysis are presented in the Table. As seen from the Table, the results of AAS and XRF analysis are comparable. Again, the main metal found in phosphogypsum is calcium. The amount of other metals is vanishingly small or below the detection limit of the method.

The BET results demonstrated that the N_2 adsorption-desorption isotherms of phosphogypsum taken from different parts of the waste were highly similar (see Fig. 9). The curves exhibit the characteristics indicative of both type II and type IV isotherms. Nonporous and macroporous materials exhibit the type II reversible isotherms,

Table. **The results of determination of a minor amount of metals in phosphogypsum using AAS and XRF analysis methods**

Metal	AAS (mass %)	XRF (mass %)
Cu	0.00064	–
Fe	0.021	0.027
Zn	0.0011	–
Sr	0.990	0.502
Mg	0.0022	–
Al	–	0.0647
Ca	19.25	20.39

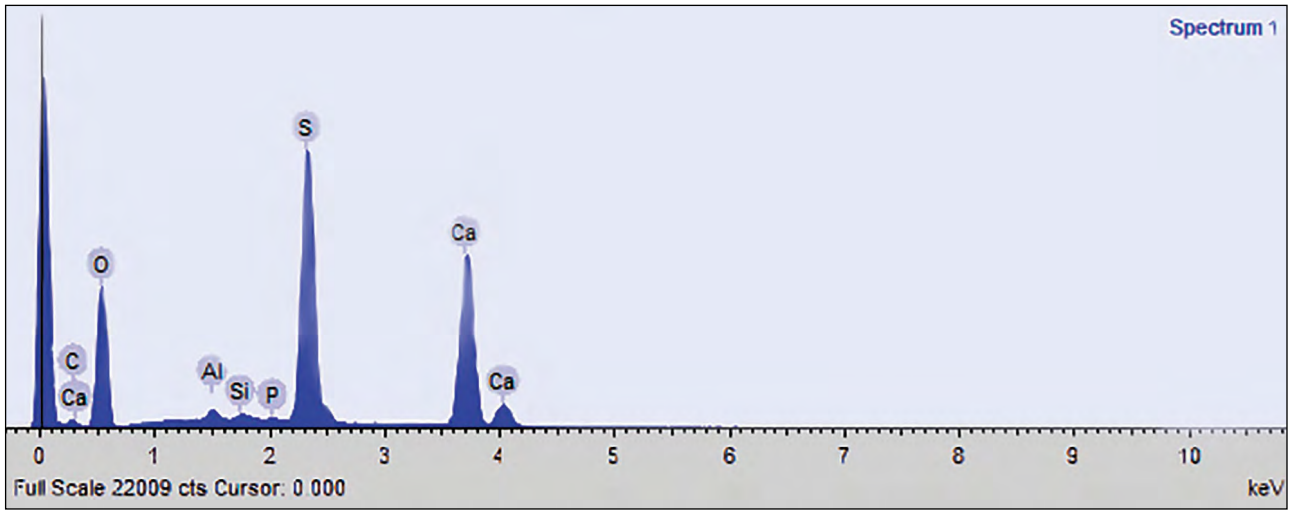

Fig. 8. EDX spectrum of the phosphogypsum sample

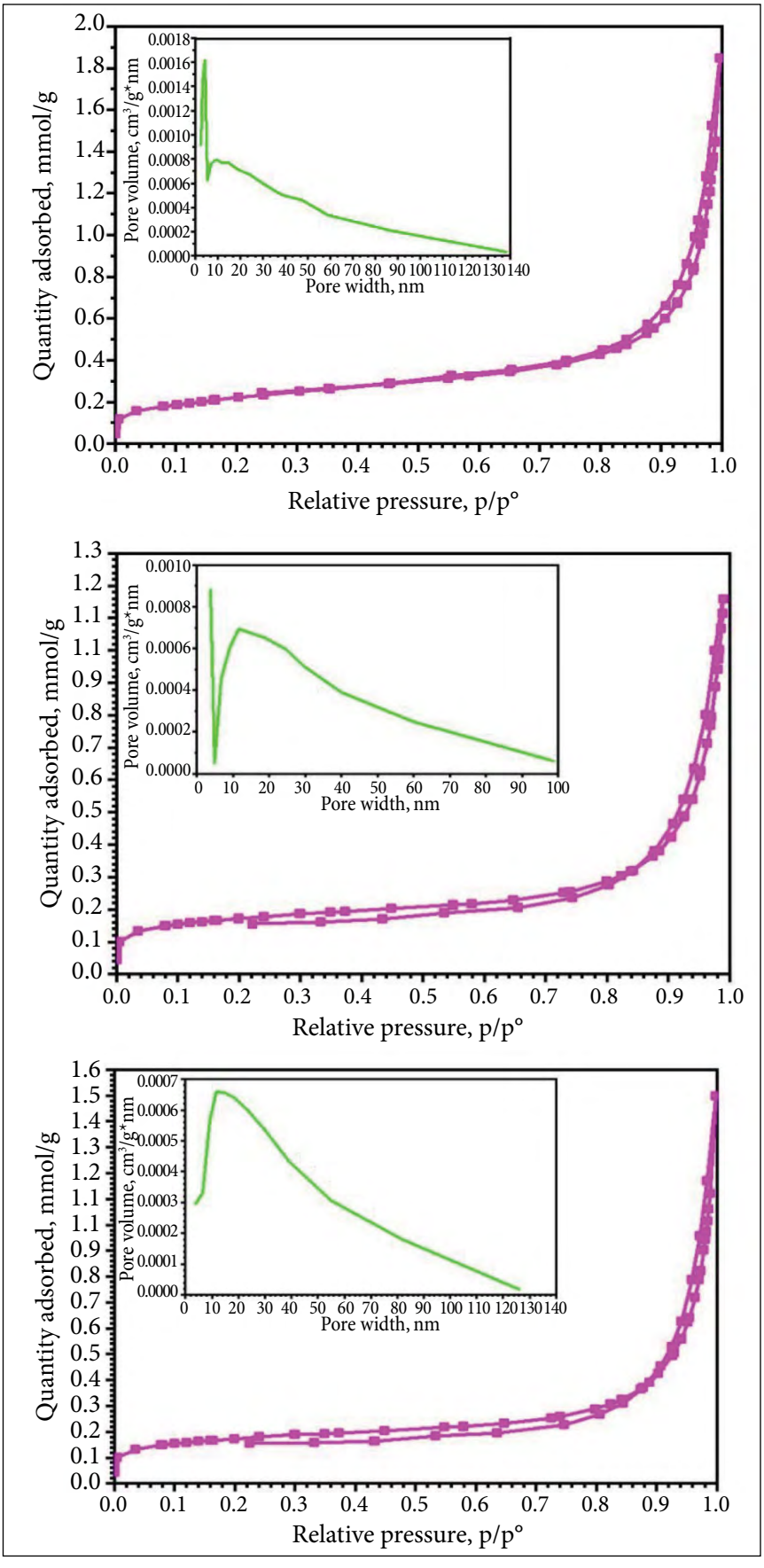

Fig. 9. N_2 adsorption-desorption isotherms of the phosphogypsum samples taken from three different parts of collected waste

which are characterised by a continuous increase in adsorption without a distinct plateau, indicating multilayer adsorption. In contrast, the type IV isotherms, which are indicative of mesoporous adsorbents, display irreversibility due to capillary condensation within the pores. At higher relative pressures, the type IV isotherms reach a variable-length saturation plateau, corresponding to the filling of mesopores and completion of adsorption. This plateau serves to distinguish the transition from multilayer adsorption to pore filling, which is characteristic of the type IV isotherms and distinguishes them from the continuous increase observed in the type II isotherms. However, no adsorption saturation is observed in the analysed samples, indicating a deviation from the typical behaviour of both type II and type IV isotherms. The analysed samples excite H3 hysteresis loops with a very narrow gap between the adsorption and desorption branches of the isotherm [14]. The inserts in Fig. 9 presents the pore size distributions obtained by the BJH method for the phosphogypsum samples. The analysis revealed a relatively wide range of pore sizes, with a prominent peak observed around 5 nm and the samples primarily comprising pores within a size range of 10–35 nm.

As was mentioned, waste phosphogypsum was used as starting materials for the fabrication of calcium hydroxyapatite ($Ca_{10}(PO_4)_6(OH)_2$; CHA) powders via a dissolution-precipitation reaction. Their diffraction patterns are displayed in Figs 10 and 11. The results of XRD analysis show that the synthesis products are slightly different depending whether disodium hydrogen phosphate (Na_2HPO_4) or a mixture of Na_2HPO_4 and sodium dihydrogen phosphate (NaH_2PO_4) were used in the synthesis protocol. The sample synthesised using Na_2HPO_4 has intensive peaks belonging to the desirable CHA phase and also to an unreacted hemihydrate $CaSO_4 \cdot 0.5H_2O$ phase even after treatment for 144 h. The amount of impurity phase decreases significantly with increasing the reaction time to 192 h. Interestingly, the duration of synthesis decreased to 144 h when CHA was synthesised using the mixture of NaH_2PO_4 and Na_2HPO_4. Finally, the polycrystalline almost single-phase $Ca_{10}(PO_4)_6(OH)_2$ was obtained from waste phosphogypsum by the developed dissolution-precipitation synthesis method. The three most intensive lines are located between $2\theta \approx 31$–$33°$ ((2 1 1) 100%, (1 1 2) 81.6% and (3 0 0) 58.9%) in the XRD pattern of the purest CHA samples. These results are in a good agreement with the reference data for $Ca_{10}(PO_4)_6(OH)_2$ (PDF [72–1243]).

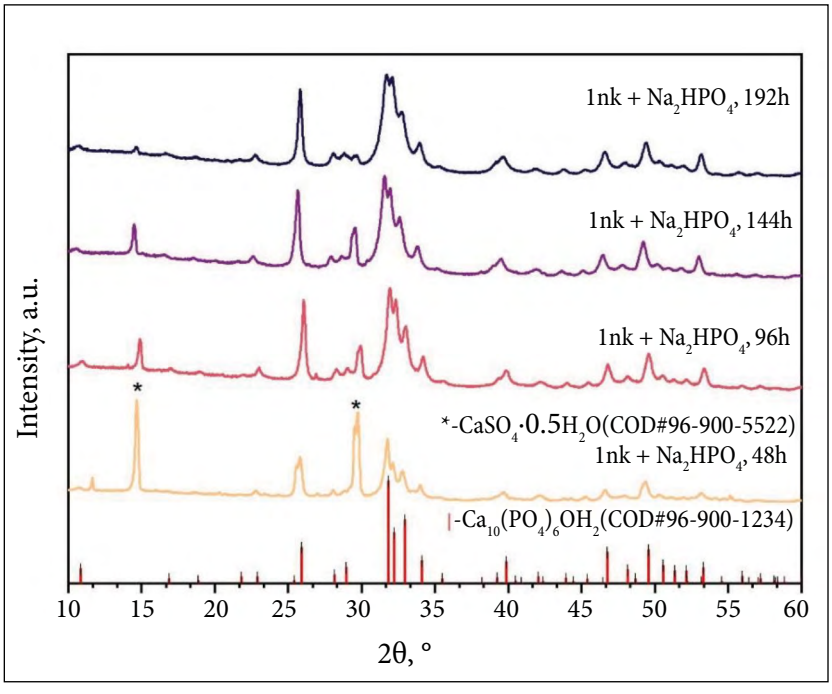

Fig. 10. XRD patterns of CHA derived from the phosphogypsum samples using Na_2HPO_4 in the dissolution-precipitation reaction

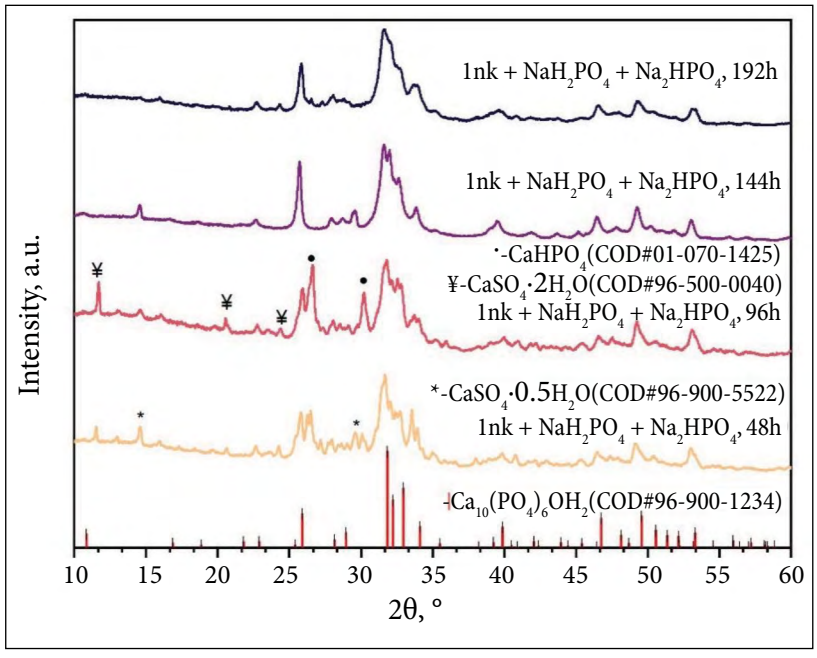

Fig. 11. XRD patterns of CHA derived from the phosphogypsum samples using the mixture of NaH2PO4 and Na2HPO4 in the dissolution-precipitation reaction

CONCLUSIONS

The phosphogypsum waste, originating from various locations within the factory dump in Kėdainiai (Lithuania), was subjected to physico-chemical characterisation using a range of methods. The results of XRD analysis showed that the main crystalline phase phosphogypsum waste is gypsum ($CaSO_4 \cdot 2H_2O$), with no evidence of the presence of other crystalline phases. From the data of TG-DSC analysis the evident transformations of gypsum to hemihydrate, soluble anhydrite and insoluble anhydrite were determined upon the heating of the phosphogypsum. The results of FTIR spectroscopy clearly supported the conclusions made from of XRD analysis data. It was determined that the surface of phosphogypsum is composed of large and differently oriented 20–30 μm in size plate-like crystals and microroads of $CaSO_4 \cdot 2H_2O$. The results of EDX analysis confirmed that Ca and S are the main elements in phosphogypsum. The calculated molar ratio of Ca:S was approximately 1. The results of the determination of metals in phosphogypsum using AAS and XRF analysis methods showed that the amount of other metals is vanishingly small or below the detection limit of the analysis method. It was concluded from the BET results that the N_2 adsorption-desorption isotherms obtained for different samples of phosphogypsum were similar. The samples were primarily comprised of pores with a size range of 10–35 nm. It was also demonstrated in this work that the phosphogypsum waste could be successfully used as precursor for the dissolution-precipitation synthesis of high quality bioceramic calcium hydroxyapatite.

Received 14 June 2024
Accepted 11 July 2024

References

1. W. Roemer, B. Steingrobe, *Sustainability*, **10**, 1166 (2018).
2. P. Vejan, T. Khadiran, R. Abdullah, N. Ahmad, *J. Control. Release*, **339**, 321 (2021).
3. N. Ahmad, M. Usman, H. R. Ahmad, M. Sabir, Z. U. R. Farooqi, M. T. Shehzad, *Env. Monit. Assess.*, **195**, 1326 (2023).
4. V. Leskeviciene, D. Nizeviciene, *Chem. Indust. Chem. Eng. Quart.*, **20**, 233 (2014).
5. J. I. Isek, L. M. Kaluderovic, N. S. Vukovic, M. Milosevic, I. Vukasinovic, Z. P. Tomic, *Clay Min.*, **55**, 63 (2020).
6. Q. J. Chen, W. J. Ding, H. J. Sun, T. J. Peng, G. H. Ma, *Energy*, **206**, 118148 (2020).
7. Y. N. Kovalev, V. N. Yaglov, T. A. Chistova, V. V. Girinsky, *Sci. Techn.*, **20**, 493 (2021).
8. H. Liu, C. C. Nie, H. P. Li, G. M. Xie, J. X. Cao, *Constr. Build. Mater.*, **347**, 128500 (2022).
9. J. Qi, H. Zhu, P. Zhou, et al., *Int. J. Env. Sci. Technol.*, **20**, 10449 (2023).

10. G. R. Lu, Z. H. Feng, Y. Xu, et al., *Agronomy-Basel*, **13**, 2726 (2023).
11. D. Yelatontsev, *J. Hazard. Mater. Lett.*, **4**, 100089 (2023).
12. A. Kyono, R. Ikeda, S. Takagi, W. Nishiyasu, *J. Mineral. Petrol. Sci.*, **117**, 015 (2022).
13. H. Boke, S. Akkurt, S. Ozdemir, E. Hale Gokturk, E. N. Caner Saltik, *Mater. Lett.*, **58**, 723 (2004).
14. R. Raiseliene, G. Linkaite, A. Zarkov, A. Kareiva, I. Grigoraviciute, *Materials*, **17**, 788 (2024).

Elžbieta Bajorinaitė, Laura Michailova, Simona Jurevičiūtė, Denis Sokol, Živilė Stankevičiūtė, Inga Grigoravičiūtė, Aivaras Kareiva

PRADINIS FOSFOGIPSO, KAIP PIRMTAKO, ATLIEKŲ PANAUDOJIMO BIOKERAMINIŲ MEDŽIAGŲ SINTEZEI ĮVERTINIMAS

S a n t r a u k a

Šiame tyrime buvo pakartotinai patikrintas ir apibūdintas skirtingais fizikiniais-cheminiais apibūdinimo metodais Kėdainiuose esančiame gamyklos sąvartyne iš įvairių vietų paimtas šalutinis gamybos produktas fosfogipsas. Rentgeno spindulių difrakcinės analizės, terminės analizės, FTIR spektroskopijos, elementinės analizės rezultatai patvirtino, kad pagrindinė kristalinė fazė fosfogipso atliekose yra gipsas ($CaSO_4 \cdot 2H_2O$). Fosfogipso paviršiaus morfologija buvo ištirta skenuojančia elektronine mikroskopija. Specifinis paviršiaus plotas nustatytas Brunauer-Emmett-Teller metodu. Medžiagų porų dydžio pasiskirstymas buvo ištirtas Barrett-Joyner-Halenda metodu. Šis tyrimas taip pat parodė, kad fosfogipso atliekos gali būti sėkmingai panaudotos kaip aukštos kokybės biokeraminio kalcio hidroksiapatito tirpinimo-nusodinimo sintezės pirmtakas.